On-line Tuning of an Efficiency-Optimized Vector Controlled Induction Motor Drive

Feng-Chieh Lin* and Sheng-Ming Yang

Department of Mechanical and Electro-Mechanical Engineering
Tamkang University
Tamsui, Taiwan 251, R.O.C.
E-mail: 890340028@s90.tku.edu.tw

Abstract

The efficiency of induction motor drive under partial load can be improved via manipulation of its field excitation. Among the numerous efficiency optimization schemes previously proposed, the scheme that uses motor power factor as the main control variable has the advantages of high sensitivity and ease of implementation. Because the optimal power factor is a function of motor speed and is sensitive to motor parameters variations, application of the power factor scheme is severely limited. In this paper, a loss-minimization control scheme that uses power factor control for vector-controlled induction motor drives is proposed. A set of near-optimal power factor commands is generated with a fuzzy logic compensator in the commissioning of the motor drive. Then an on-line tuning controller is used to adjust the power factor command to its optimal value when the motor is at normal operations. The scheme is practical for implementation and does not require a priori knowledge of motor parameters.

***Key Words*:** Induction Motor, Loss Minimization, Vector Control, Fuzzy Logic, On-line Tuning.

1. Introduction

Approximately half of the power in the world today is consumed by electric motors, and the majority of them are induction motors. Because the efficiency of an induction motor varies significantly with its operating condition, energy savings by reducing operating loss can be obtained with optimal control strategies. The operating loss in an induction motor includes: 1) stator and rotor copper losses, 2) core losses and 3) mechanical losses. Under light loads, motor efficiency decreases due to an imbalance between the copper and the core losses. Hence, energy saving can be achieved by proper selection of the flux level in the motor.

Many minimum-loss control schemes have been reported previously. These schemes can be separated into three categories. 1) Search method [1-5]. The controller searches for the operating point where the input power is at a minimum while keeping the motor output power constant. Because the relationship between input power and flux near the minimum-loss point is fairly flat, the input power must be measured accurately to prevent oscillatory response in the control. 2) Loss model method [6-10]. Because motor losses in the direct and the quadratic axes are balanced when the motor is at its minimum-loss point, a feedback controller can be used to force the motor to operate at this point. A loss model is required for loss calculation in this scheme. 3) Power factor method [11-12]. This scheme utilizes an interesting property of induction motor that when the motor is running at constant speed, the motor power factor is constant regardless of load when operating at its minimum-loss point. Thus at any speed, motor power factor can be controlling to the value where

operating loss is minimal corresponding to this speed. The power factor control scheme has the advantage that the controller can be stabilized easily and the motor parameter information is not required. However, generation of the optimal power factor commands remains tedious and restrictive because empirical, trial and error methods are generally used.

In this paper, a loss-minimization scheme based on motor power factor for vector-controlled induction motor drives is proposed. A set of near-optimal power factor command is generated with a fuzzy logic compensator in the commissioning of the motor drive. Then an on-line tuning controller is used to adjust the power factor command to its optimal value when the motor is at normal operations.

2. Motor Loss Model

The d-q equations for a three-phase squirrel cage induction motor in a synchronous rotating frame can be expressed as

$$v_{qs}^e = r_s i_{qs}^e + p\lambda_{qs}^e + \omega_e \lambda_{ds}^e \tag{1}$$

$$v_{ds}^e = r_s i_{ds}^e + p\lambda_{ds}^e - \omega_e \lambda_{qs}^e \tag{2}$$

$$0 = r_r i_{qr}^e + p\lambda_{qr}^e + (\omega_e - \omega_r)\lambda_{dr}^e \tag{3}$$

$$0 = r_r i_{dr}^e + p\lambda_{dr}^e - (\omega_e - \omega_r)\lambda_{qr}^e \tag{4}$$

where v_{qs}^e, v_{ds}^e, i_{qs}^e, i_{ds}^e, i_{qr}^e, i_{dr}^e, λ_{qs}^e, λ_{ds}^e, λ_{qr}^e, λ_{dr}^e are the *q-d* axis stator voltages, stator and rotor currents, stator and rotor flux, respectively; r_s and r_r are the stator and rotor resistance, respectively; ω_e is the frequency, ω_r is the rotor electrical speed, and p is the derivative operator. The operating loss of an induction motor is composed of the stator and rotor copper losses, the core losses and the mechanical losses. Mechanical losses are neglected since they are small compared with other losses. Core losses are made up of Eddy current and hysteresis losses. Since Eddy current loss and hysteresis loss can be modeled as a function proportional to ω_e and a function proportional to the square of ω_e [13], respectively, the total operating loss is

$$P = \frac{3}{2}\left[\left(i_{qs}^{e\,2} + i_{ds}^{e\,2}\right)r_s + \left(i_{qr}^{e\,2} + i_{dr}^{e\,2}\right)r_r + K_h\omega_e\lambda_m^{e\,2} + K_e\omega_e^{\,2}\lambda_m^{e\,2}\right] \tag{5}$$

where λ_m^e is the air-gap flux, K_e and K_h are the Eddy current and hysteresis loss coefficients, respectively. When the motor is running under the rotor flux field orientation and at steady state, $i_{dr}^e = 0$ and $i_{qr}^e = -\frac{L_m}{L_r} i_{qs}$. Hence, λ_m^e can be eliminated from Eq. (5), and the loss becomes

$$P = \frac{3}{2}\left[\left(i_{qs}^{e\,2} + i_{ds}^{e\,2}\right)r_s + \frac{L_m^{\,2}}{L_r^{\,2}} i_{qs}^{e\,2} + \left(K_h\omega_e + K_e\omega_e^{\,2}\right)\left(\frac{L_r^{\,2}L_m^{\,2}}{L_r^{\,2}} i_{qs}^{e\,2} + L_m^{\,2} i_{ds}^{e\,2}\right)\right] \tag{6}$$

where L_r and L_m are the rotor and the mutual inductance, respectively.

3. Principle of Minimum-Loss Control

In this section, a minimum-loss control scheme that uses power factor as the primary control variable is presented. The definition of motor power factor in d-q frame is

$$PF = \cos\theta = \frac{V_{qs}^e i_{qs}^e + V_{ds}^e i_{ds}^e}{\sqrt{V_{qs}^{e\,2} + V_{ds}^{e\,2}}\sqrt{i_{qs}^{e\,2} + i_{ds}^{e\,2}}} \tag{7}$$

The minimum-loss power factor, *PF**, as a function of motor speed, rotor flux and torque can be expressed as [12]

$$PF^* = \frac{\frac{4\omega_r}{3p} + \frac{16}{9p^2}\left[r_s\frac{L_r^{\,2}}{L_m^{\,2}} + r_r\right]\sqrt[2]{\frac{K2}{K_1}} + \frac{r_s}{L_m^{\,2}}\sqrt[2]{\frac{K_1}{K_2}}}{\sqrt{\left[\sqrt[4]{\frac{K_1}{K_2}}a_0\omega_r + a_1\sqrt[4]{\frac{K_2}{K_1}}\right]^2 + \left[-a_2\sqrt[4]{\frac{K_1}{K_2}} + a_3\sqrt[4]{\left(\frac{K_2}{K_1}\right)^3} + a_4\sqrt[4]{\frac{K_2}{K_1}}\omega_r\right]^2}\sqrt{a_5^{\,2}\sqrt[2]{\frac{K2}{K_1}} + a_6^{\,2}\sqrt[2]{\frac{K_1}{K_2}}}} \tag{8}$$

where a_0~a_6 are constants and their values can be found in Appendix A. As indicated in Eq. (8), *PF** is a function of motor parameters and ω_r only, it is not a function of motor load torque.

The above results are illustrated by Figure 1, where the motor operating loss and *PF* vs. i_{ds}^e plots under various motor torques for a typical one horsepower motor running at 900 rpm are shown. The motor parameters can be found in Appendix B. As can be seen in Figure (1a), the minimum-loss points are indicated by 'o', varied for different motor torque (T_e). But the power factors at the minimum-loss power points shown in Figure (1b) are identical regardless of T_e. This is consistent with the result indicated by Eq. (8). The

minimum-loss power factors are generally located near the region where the slope of the power factor vs. i_{ds}^e curve is steepest, i.e. negatively largest. In addition, the minimum-loss power factors are located away from the peak of the power factor vs. i_{ds}^e curves except at very low speeds.

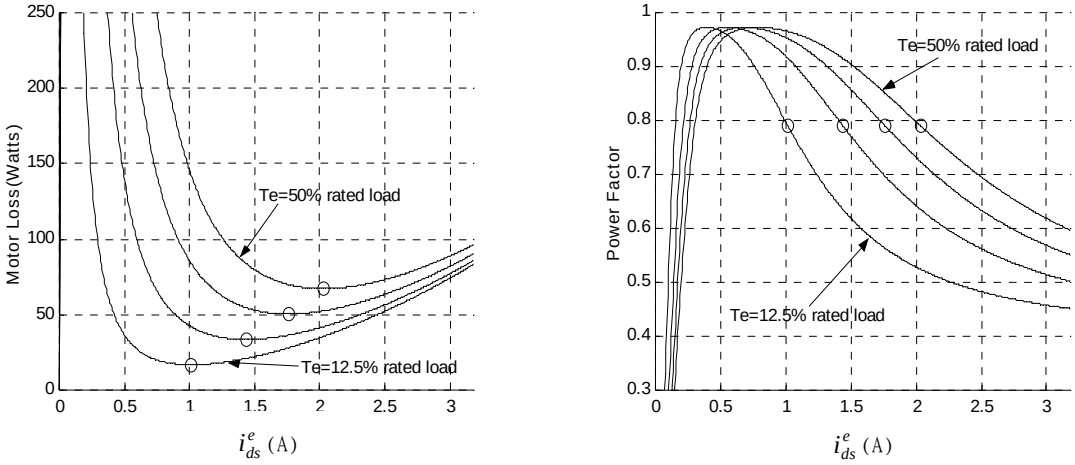

(a) (b)

Figure 1. (a) Operation loss and (b) power factor vs. i_{ds}^e at various motor torque for a typical 1 HP motor running at 900 rpm

Note that if separating the motor loss shown in Eq. (6) into a quadratic and a direct axis component, then

$$W_q = \left[r_s + \frac{L_m^{\,2}}{L_r^{\,2}} r_r + (K_h \omega_e + K_e \omega_e^{\,2}) \frac{L_{lr}^{\,2} L_m^{\,2}}{L_r^{\,2}} \right] i_{qs}^{e\,2} \tag{9}$$

$$W_d = \left[r_s + (K_h \omega_e + K_e \omega_e^{\,2}) L_m^{\,2} \right] i_{ds}^{e\,2} \tag{10}$$

where W_q and W_d are the q-axis and the d-axis loss. Let $A = i_{qs}^e / i_{ds}^e$, the minimum-loss condition for A can be obtained by dividing i_{qs}^e i_{ds}^e into Eq. (6) and taking the derivative with respect to A on the result.

$$\left[r_s + \frac{L_m^{\,2}}{L_r^{\,2}} r_r + (K_h \omega_e + K_e \omega_e^{\,2}) \frac{L_{lr}^{\,2} L_m^{\,2}}{L_r^{\,2}} \right] i_{qs}^{e\,2} = \left[r_s + (K_h \omega_e + K_e \omega_e^{\,2}) L_m^{\,2} \right] i_{ds}^{e\,2} \tag{11}$$

Equation (11) implies that W_q equals W_d when the motor is running at the minimum-loss point, and the optimal current ratio A^* is

$$A^{*2} = \frac{L_m^{\,2} K_e \omega_e^{\,2} + L_m^{\,2} K_h \omega_e + r_s}{\frac{L_{lr}^{\,2} L_m^{\,2}}{L_r^{\,2}} (K_e \omega_e^{\,2} + K_h \omega_e) + \frac{L_m^{\,2}}{L_r^{\,2}} r_r + r_s} \tag{12}$$

In the above equation, A^* is not a function of T_e. This is a property similar to PF^* shown in Eq. (8). For verification, current ratio vs. i_{ds}^e plots under various motor torques for the one horsepower motor running at 900 rpm are calculated and shown of Figure 2. The minimum loss points, indicated by 'o', are identical regardless of T_e. This result will be used to design the on-line tuning controller in Section 5.

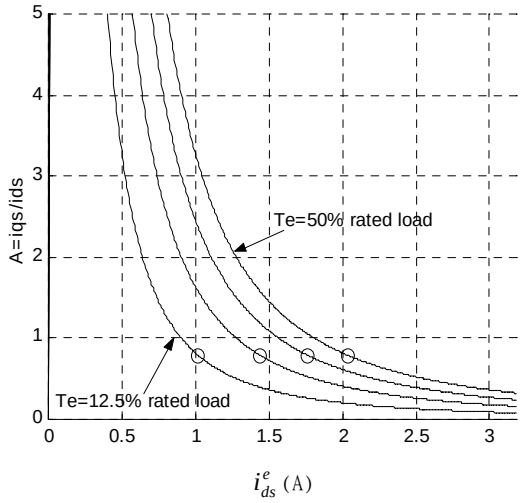

Figure 2. Current ratio vs. i_{ds}^e at various motor torque for a typical 1 HP motor running at 900 rpm

4. Power Factor Control

A minimum-loss power factor control for vector-controlled induction motor drives can be realized using the previous results. Figure 3 shows the block diagram of the controller. For convenience, the motor is controlled with a velocity controller which manipulating i_{qs}^e to get the desired motor speed. The power factor controller is indicated with dotted lines. The relationship between PF^* and speed is calculated in advance and stored as the reference for the

controller. Motor power factor is calculated from the measured motor terminal voltages and currents. The error between the reference and the measured power factor is regulated via a PI controller to zero by manipulating i_{ds}^{e}.

Although the minimum-loss power factor can be calculated with Eq. (8), the calculation is very difficult due to the complexity of the equation and a priori knowledge of motor parameters including K_h and K_e is required. This paper proposed a scheme that combines fuzzy logic technique and on-line tuning to obtain the optimal power factor command. The block diagram of the command generator is shown in Figure 4. In the commissioning of the motor drive, a fuzzy logic compensator is used to generate a set of near-optimal power factor commands, i.e. *PF_o*, according to the measured motor parameters. Afterwards, when the motor is in normal operations, an on-line tuning controller is used to adjust the power factor command to its optimal value. The power factor correction output from the tuning controller is denoted as *PF_t*. Detail of this scheme is described in the following sections.

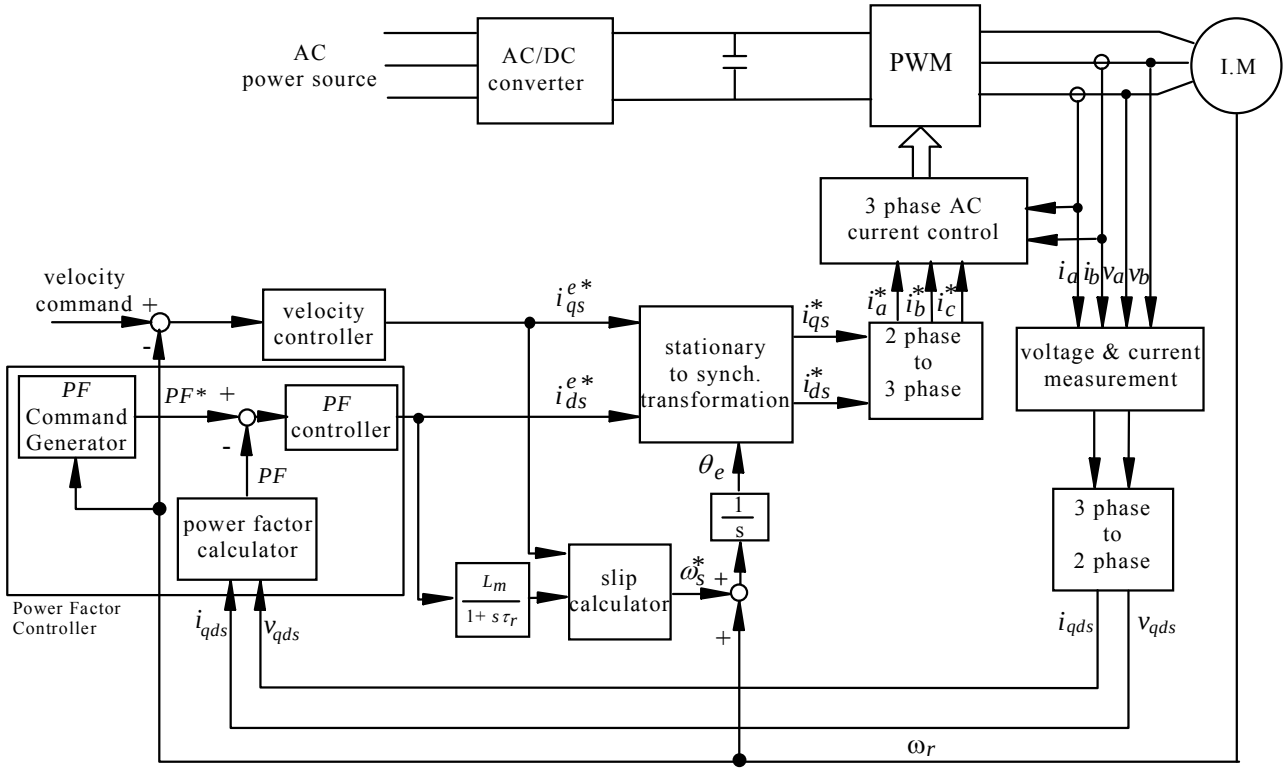

Figure 3. Block diagram for the minimum-loss control system

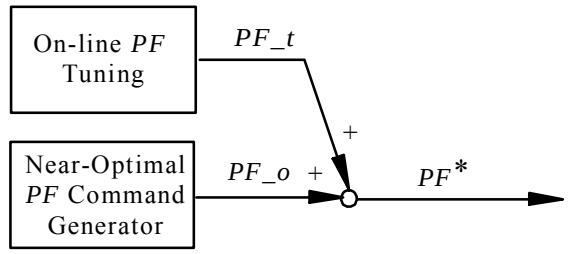

Figure 4. Block diagram for the optimal power factorcommand generator

5. Near-Optimal *PF* Command Generation with Fuzzy Logic

The near-optimal *PF* command is generated based on the derivative of *PF* vs. i_{ds}^{e} curves shown in Figure 1 (b). For the one horsepower motor, its power factor derivative vs. i_{ds}^{e}, i.e. $\partial(PF)/\partial i_{ds}^{e}$ vs. i_{ds}^{e}, is shown in Figure 5. Let the minimum of $\partial(PF)/\partial i_{ds}^{e}$ vs. i_{ds}^{e} be *PF_d* for convenience, and the minima of these curves are denoted with '*'. It can be shown that *PF_d* is a function of motor speed only when iron saturation is neglected, a property *PF** and *A** also possessed. For comparison, the '*' points were superimposed on Figure (1b) and then shown in Figure 6. It can be seen

that the '*' points are very close to the minimum-loss points. To verify if *PF** can be substituted by *PF_d*, both *PF** and *PF_d* vs. motor speed for the 1 hp motor were calculated and shown in Figure 7. The two curves are very close to each other at medium and low speeds, but have noticeable discrepancies at high speeds. Therefore *PF** can't be substituted by *PF_d* especially at high speed.

In this paper, however, we still propose to use *PF_d* to approximate *PF** but with compensation. The main reason is that *PF_d* can be found by using automatic measurements conveniently, and the measurement can be performed in the absence of load [12]. This has greatly simplified the measurement procedures and allowed them to be implemented as part of the auto-commissioning of the motor drive. Because the error between *PF_d* and *PF** is a nonlinear function of motor speed, also varying with motor size, a fuzzy logic compensator is employed to compensate for the error. Figure 8 illustrates the basic structure of the proposed fuzzy compensator. The compensator uses *PF_d* and ω_r as its input, and the output is a correction term, i.e. *PF_c*, for the power factor command. Details of the fuzzy logic design can be found in [12].

Figure 9 shows the simulated *PF_o*, *PF_c*, and *PF_d* for 1 hp motor, respectively. It can be seen that all the calculated power factors are very close to the theoretical minimum-loss power factors. The largest error was around 0.03 for the motor. In practice this error can be neglected since the loss vs. i_{ds}^e curve is flat near the minimum-loss point. Note that the motors parameters used for the calculation in this section can be found in Appendix B.

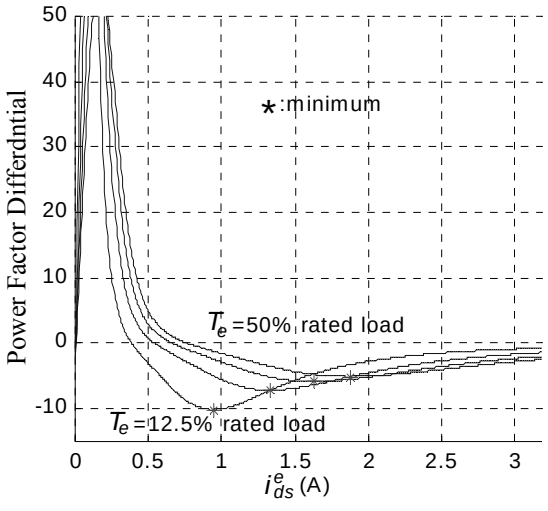

Figure 5. $\partial(PF)/\partial i_{ds}^e$ vs. i_{ds}^e, '*' indicates the minimum value

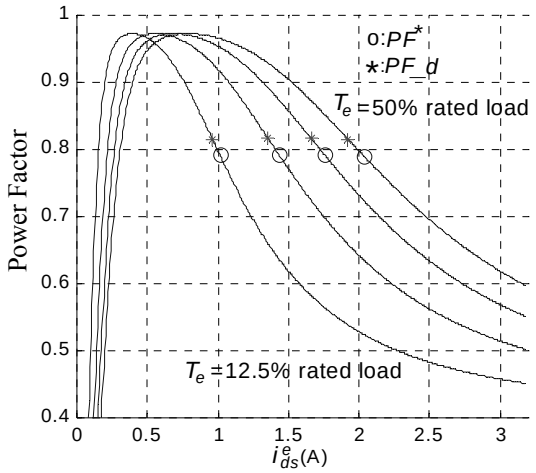

Figure 6. Overlapping of *PF_d* on Figure (1b)

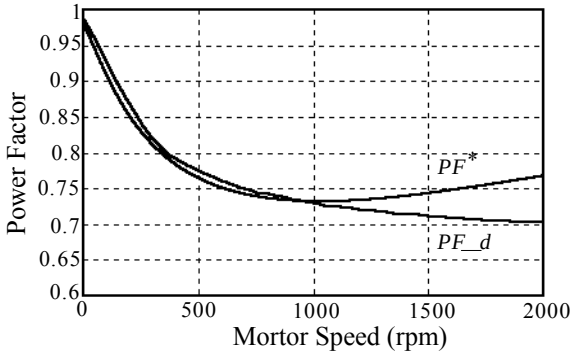

Figure 7. Comparisons of PF^* and PF_d vs. motor speed for the 1 hp motor

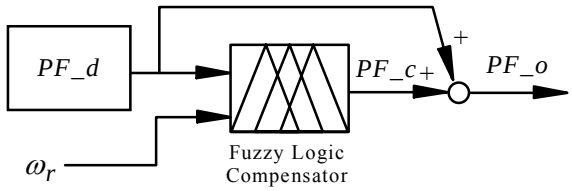

Figure 8. Block diagram for the fuzzy logic power factor compensator

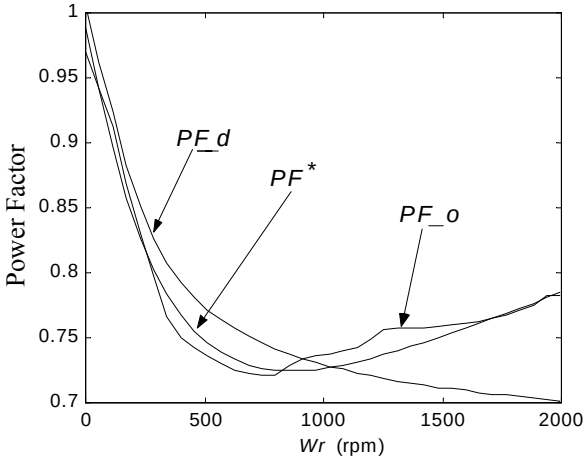

Figure 9. Comparisons of the optimal and the compensated power factor for 1 HP motors

6. On-line *PF* Command Tuning

As shown in the previous section, there are still some errors in *PF_o* even with the fuzzy compensation. An on-line tuning controller is designed to adjust *PF_o* to its optimal value. In general, it is a reasonable assumption that K_e equals K_h [13]. Calculations have also shown that substantial variations in these constants have little impact on the performance of the tuning controller. Therefore, let $K = K_e = K_h$, then Eq. (11) can be rewritten as

$$K = \frac{r_s\left(1 - A^2\right) - \dfrac{L_m{}^2}{L_r{}^2} r_r A^2}{\dfrac{L_{lr}{}^2 L_m{}^2}{L_r{}^2}\left(\omega_e{}^2 + \omega_e\right)A^2 - L_m{}^2\left(\omega_e{}^2 + \omega_e\right)} \tag{13}$$

The above equation is valid only when the motor is operating at the minimum-loss conditions, moreover, it shows that *K* is a function of *A* and ω_e. In another words, when both *A* and ω_e are fixed, then *K* is constant when the motor is operating at the minimum-loss condition. In contrast, *K* is not constant when the motor is not operating at the minimum-loss condition. Therefore *K* can be used to determine if the motor is operating at minimum-loss conditions. The proposed on-line tuning controller is designed based on this principle.

Figure 10 shows the block diagram of the proposed tuning controller. The inputs are ω_e, i_{ds}^e and i_{ds}^e; they are required for the calculation of *K*. The output is *PF_t*; it is used to adjust *PF_o* to its optimal value. The intermediate term, $\triangle K$, is the differential of *K* calculated from two distinct *A* and ω_e operating conditions. Note that tuning can be carried out only when both *A* and ω_e are fixed. Also, since minimum-loss *A* for any speed is unique, $\triangle K$ can be calculated only when the motor is operating at different ω_e.

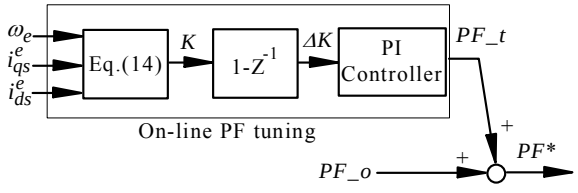

Figure 10. Block diagram of the on-line tuning controller

Figure 11 shows a typical simulation result of the on-line tuning controller for the one horsepower motor. The motor was controlled to run at 1000 and 1500 rpm in succession. The initial minimum-loss power factor commands and *K*'s for the two speeds were set to 0.65, 0.7 and 0, 0.0005, respectively. The correct power factor commands are 0.73 and 0.75 for the two speeds. It can be seen that both power factor commands and *K* slowly converging to fixed values after on-line tuning was activated. After about 400 seconds, *K* settled down to approximately 0.00013, which is the correct value. The power factor commands for both speeds also converged to their minimum-loss values.

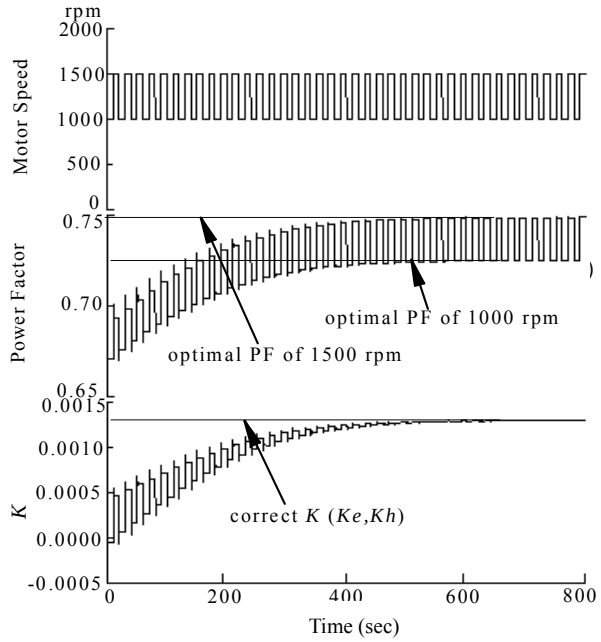

Figure 11. Simulation results of the on-line tuning control

7. Experimental Results

The on-line tuning control scheme proposed in the previous section was implemented with a PC and DSP based system for experimental verifications. Figure 12 shows the experimental setup. A PC equipped with Pentium III microprocessor performed the online tuning control and fuzzy logic *PF** calculations. A TMS320C240 DSP, which linked to PC through parallel interface, performed the power factor and the other motor control loops. The parameters of the 1 hp induction motor used in the experiments can be found in Appendix B. Vector control for induction motor was implemented in the DSP to assist the verification of the minimum-loss control scheme. Both *d*- and *q*-axis voltages and currents were measured and filtered so that only the fundamental components were read by the DSP for power factor calculation. Information communicated between PC and DSP are shown in Figure 12.

Figure 13 shows the experiment results of the on-line tuning when the motor was running up and down between 1000 and 1500 rpm. Because this

experiment was intended to verify the simulation results shown in Figure 11, the initial minimum-loss power factor commands and *K*'s for the two speeds were also set to approximately 0.65, 0.7 and 0, 0.0005, respectively. Again, the correct power factor commands are 0.73 and 0.75 for these speeds. As can be seen in this figure, the power factor commands calculated matched the optimal power factor, and *K* slowly converging to its correct value.

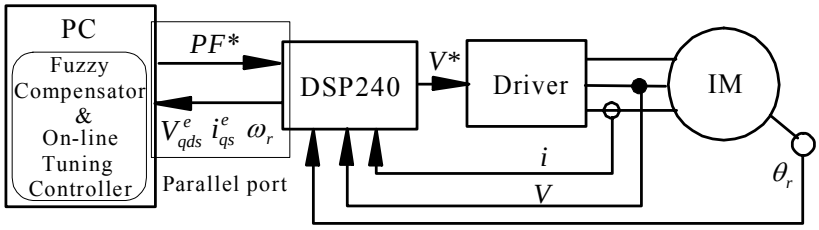

Figure 12. Experimental system

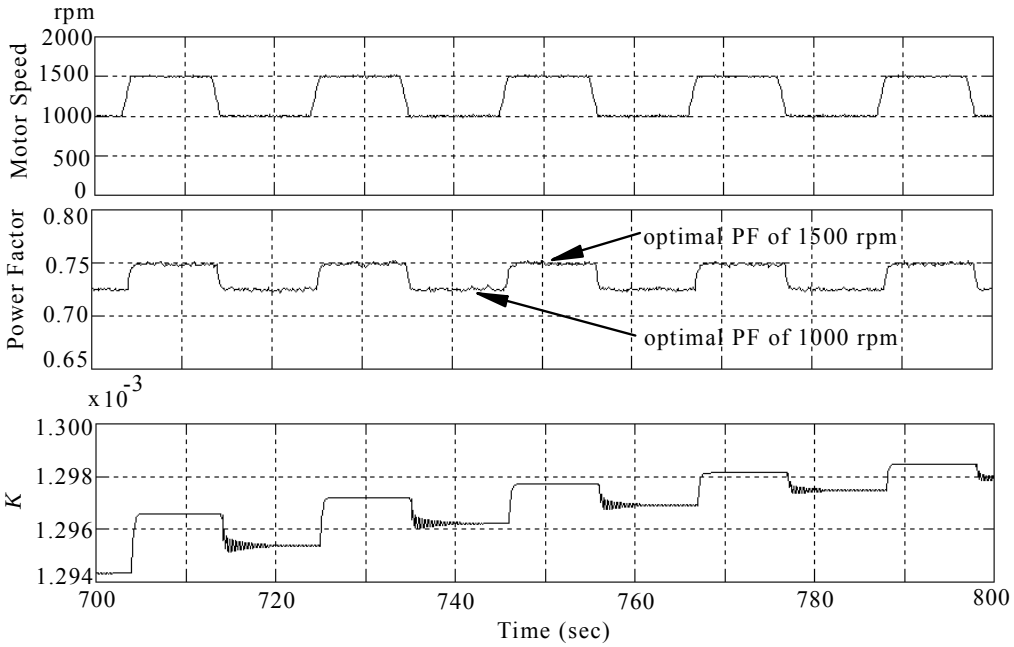

Figure 13. Experiment results of the on-line tuning control

8. Conclusions

A loss-minimization control scheme that uses power factor control for vector-controlled induction motor drives is proposed in this paper. The control scheme utilizes motor power factor as the main control variable and manipulates the magnetizing current in order for the motor to operate at its minimum-loss point. A scheme to acquire the optimal power factor command is also proposed. A set of near-optimal power factor commands is generated with a fuzzy logic compensator in the commissioning of the motor drive. Then an on-line tuning controller is used to adjust the power factor command to its optimal value when the motor is at normal operations. The scheme is practical for implementation and does not require a priori knowledge of motor parameters. The simulation and the experimental results have confirmed the effectiveness of the proposed scheme in the generation of minimum-loss power factor commands.

Acknowledgments

We gratefully acknowledge the support for this research by the National Science Council, Taiwan, R. O. C., under grant: NSC 90-2213-E-032-021.

Appendix A

$$a_0 = (\frac{L_m}{L_r} + \sigma \frac{L_s}{L_m}),$$

$$a_1 = \frac{4}{3P}(r_r(\frac{L_m}{L_r} + \sigma \frac{L_s}{L_m}) + \frac{L_r}{L_m} r_s), \quad a_2 = \frac{r_s}{L_m},$$

$$a_3 = \frac{16\sigma}{9P^2}\frac{L_s L_r r_r}{L_m}, \quad a_4 = \frac{4\sigma}{3P}\frac{L_s L_r}{L_m},$$
$$a_5 = \frac{4}{3P}\frac{L_r}{L_m}, \quad a_6 = \frac{1}{L_m}$$

Appendix B

The motor is three-phase, four-pole, 66Hz, 2000 rpm, the parameters are:

	r_s (ohm)	r_r (ohm)	L_s (H)	L_r (H)	L_m (H)	K_h	K_e	Voltage
1 hp	5.23	2.4	0.1908	0.1940	0.1876	87e-5	87e-5	220

References

[1] Ta, C. M. and Hori, Y., "Convergence Improvement of Efficiency-Optimization Control of Induction Motor Drives," *IEEE Transactions on Industry Applications*, Vol. 37, pp. 1746-1753 (2001).

[2] Bose, B. K., Patel, N. R. and Rajashekara, K., "A Neuro-Fuzzy-Based On-Line Efficiency Optimization Control of a Stator Flux-Oriented Direct Vector-Controlled Induction Motor Drive," *IEEE Transactions on Industrial Electronics*, Vol. 44, pp. 270-273 (1997).

[3] Sousa, G. C. D., Bose, B. K. and Cleland J. G., "Fuzzy Logic Based On-Line Efficiency Optimization Control of an Indirect Vector-Controlled Induction Motor Drive," *IEEE Transactions on Industrial Electronics*, Vol. 42, pp. 192-198 (1995).

[4] Huang, T. C. and El-Sharkawi, M. A., "Induction Motor Efficiency Maximizer Using Multi-layer Fuzzy Control," *Intelligent Systems Applications to Power Systems, Proceedings, ISAP '96, International Conference on*, Orlando, FL, U.S.A., pp.109-113 (1996).

[5] Blaabjerg, F. and Pedersen, J. K., "An Integrated High Power Factor Three-Phase AC-DC-AC Converter for AC-Machines Implemented in One Microcontroller," *IEEE Power Electronics Specialists Conference*, Seattle, WA, U.S.A., pp. 285-292 (1993).

[6] Poirier, E., Ghribi, M. and Kaddouri, A., "Loss Minimization Control of Induction Motor Drives Based on Genetic Algorithms," *Electric Machines and Drives Conference, IEEE International*, Cambridge, MA, U.S.A., pp. 475-478 (2001).

[7] Anderson, H. R. and Pedersen, J. K., "On the Energy Optimized Control of Standard and High-Efficiency Induction Motors in CT and HVAC Applications," *Conference Record of the 1997 IEEE IAS Annual Meeting*, New Orleans, LA, U.S.A., pp. 621-628 (1997).

[8] Fernandez-Bernal, F., Garcia-Cerrada, A. and Faure, R., "Model-Based Loss Minimization for DC and AC Vector-controlled Motors Including Core Saturation," *IEEE Transactions on Industry Applications*, Vol. 36, pp. 755-763 (2000).

[9] Taniguchi, S., Yoshizumi, T. and Matsuse, K., "A Method of Speed Sensorless Control of Direct-Field-Oriented Induction Motor Operating at High Efficiency with Core Loss Consideration," *Applied Power Electronics Conference and Exposition*, Vol. 2, pp. 1244-1250 (1999).

[10] Lu, X. and Wu, H., "Maximum Efficiency Control Strategy for Induction Machine," *Electrical Machines and Systems*, Vol. 1, pp. 98-101 (2001).

[11] Anderson, H. R. and Pedersen, J. K., "Low Cost Energy Optimized Control Strategy for a Variable Speed Three-Phase induction Motor," *Proceedings of the 1996 IEEE-PESC*, Maggiore, Italy, Vol. 1, pp. 920-924 (1996).

[12] Yang, S. M. and Lin, F. C., "Loss-Minimization Control of Vector-Controlled Induction Motor Drives," *Journal of the Chinese Institute of Engineers*, Vol. 26, pp. 37-45 (2003).

[13] Kirschen, D., Novotny, D. W. and Suwanwisoot, W., "Minimizing induction Motor Losses by Excitation Control in Variable Frequency Drives," *IEEE Trans. on IAS*, Vol. 20, pp. 1244-1250 (1984).

Manuscript Received: Jan. 15, 2003
and Accepted: Mar. 20, 2003